Transportation Research Part C 18 (2010) 471–488

Contents lists available at ScienceDirect

Transportation Research Part C

journal homepage: www.elsevier.com/locate/trc

Parameter-dependent modeling of freeway traffic flow

Tamás Luspay [a], Balázs Kulcsár [b], István Varga [a,*], József Bokor [a]

[a] Systems and Control Laboratory, Computer and Automation Research Institute, Hungarian Academy of Sciences, H-1111, Budapest, Kende u. 13-17, Hungary
[b] Delft Center for Systems and Control, Faculty of Mechanical, Maritime and Materials Engineering, Delft University of Technology, 2628 CD Delft, Mekelweg 2, The Netherlands

ARTICLE INFO

Article history:
Received 3 April 2009
Received in revised form 4 September 2009
Accepted 8 September 2009

Keywords:
Freeway traffic flow modeling
Linear Parameter Varying systems

ABSTRACT

In the paper a novel non-linear modeling formalism is suggested for freeway traffic flow. A second-order macroscopic model has been transformed into a Linear Parameter Varying (LPV) model. The paper proposes two LPV descriptions for traffic modeling: the first one covers completely the non-linear macroscopic dynamics, while the second one is an approximate description. Real test field topology and measurement data are used for validating the proposed modeling methodology. Simulation examples are given to compare real detector measurements, non-linear and the parameter-dependent responses.

1. Introduction and motivation

Congested roads induce environmental and economic losses and have become one of the biggest problems in recent years to be solved. Engineers and researchers from the field of transportation and control theory work on developing effective solutions accordingly (Papageorgiou, 1983).

Modern systems and control theory can improve the level of freeway monitoring and surveillance by the results of estimation, filtering and control. Observation or filtering means the reconstruction of the unmeasured variables from noisy measurements, multiplying the available data sets in freeways. Control methods are considered as mathematical algorithms for the adequate intervention into the system's dynamics. Modern, traffic-responsive control techniques are based on dynamical models, adjusting on-line control inputs, focusing on the control of merging traffic by ramp metering and the control of mainstream flow via variable speed limits (Papageorgiou, 2003).

The question of an adequate model of the physical process is of capital importance during the observer and controller design. Creating a precise freeway traffic model is a great challenge, due to the complex dynamics of the real process. At the same time, there exists a tradeoff between the complexity of model and its adaptation in real life applications.

The present traffic modeling approaches can be classified according to their level of detail. In microscopic models individual vehicles are distinguished (Leutzbach, 1988), while macroscopic techniques use aggregated variables to describe traffic. Macroscopic models can be grouped as first- and second-order models. First-order models use the continuum equation to describe the evolution of traffic density, while second-order models apply also a momentum equation for speed evolution (Hoogendoorn and Bovy, 2001). Comparative analysis shows that second-order macroscopic models reproduce freeway phenomena with accuracy higher than the first-order ones, therefore mainly these models are in the focus of freeway control and estimation (Michalopoulos et al., 1992), at the same time the complexity of these models may increase computational complexity in model based controller design. Moreover, solutions obtained from second-order models can be in contrast with the real process (Daganzo, 1995).

* Corresponding author. Tel.: +36 12796173; fax: +36 14667483.
E-mail addresses: tluspay@sztaki.hu (T. Luspay), b.a.kulcsar@tudelft.nl (B. Kulcsár), ivarga@sztaki.hu (I. Varga), bokor@sztaki.hu (J. Bokor).

0968-090X/$ - see front matter
doi:10.1016/j.trc.2009.09.005

Freeway models can be the basis of traffic surveillance and traffic designs, through analysis, identification, estimation and control. These methods are based on the mathematical model of the process, therefore, non-linear differentia equations imply the use of non-linear techniques (Isidori, 1995). The non-linear methods developed are large enough, but some drawbacks of the non-linear system class are known. System analysis may lead to hard computations, especially in case of systems with high state-space dimension. The developed estimator or controller design methods are not valid for all kind of non-linear systems, the design methods are not systematic in contrast to linear systems (Hangos et al., 2004).

In order to handle non-linearities in freeway applications, off- and on-line linearization are used. The advantage of off-line linearization is the resulting linear description, which allows the application of systematic linear techniques (Papageorgiou et al., 1991). The disadvantage of methods like this is reduced accuracy whenever the real traffic state significantly disagrees with the chosen operation point, since in this case the linear plant is not valid. Another possible solution is on-line linearization around a current point (Wang and Papageorgiou, 2005; Hegyi et al., 2005), giving different linearized models in the whole range of operation. On the other hand, systematic design, tractable numerical algorithms and stability guarantee are not necessarily represented by these methods.

In recent years LPV formalism has been a promising approach for non-linear control theory (Wu, 1995; Rugh and Shamma, 2000). The LPV description preserves the linear structure for non-linear systems by introducing the concept of scheduling parameters. Non-linearities can be rewritten as time-varying parameters. The resulting structure will be linear in the states with parameter-dependent system matrices. The scheduling parameter vector is a known, continuous and time-dependent function, which makes the evaluation of the transformed non-linear system at every single k possible. In the particular case when the parameter vector coincides (partially or entirely) with the state vector, the system is called quasi-Linear Parameter Varying (qLPV) system (Shamma and Athans, 1990). It was shown that non-linear systems could be cast into an LPV form in several ways, therefore, the LPV model is not unique (Shamma and Cloutier, 1993).

The aim of the paper is to introduce a control-oriented modeling technique for freeways, uniting the accuracy of non-linear models with the powerful analysis and design methods of linear systems, by introducing the concept of Linear Parameter Varying (LPV) systems. To rewrite the non-linear macroscopic freeway model into an qLPV form, a transformation method has been developed for a class of non-linear discrete time systems.

The paper presents a special reformulation of the second-order macroscopic traffic model in four sections. After the introductory section, preliminaries regarding freeway traffic models, and theory of LPV formalism are summarized and the problem is stated. The next section presents a solution for the parameter-dependent modeling of freeway flow. First, the idea of an integral transformation for the freeway model in question is introduced in Section 3.1. In order to apply this transformation, a change in the variables is needed, which is described under Section 3.2. Sections 3.3 and 3.4 present two different (an exact and an approximate) LPV models, both obtained by applying the integral transformation. Finally, in Section 4 numerical results are given for a freeway stretch in The Netherlands. The section gives the detailed description of exact and approximate LPV structures and shows the comparative simulation results of the models derived, based on detector measurements.

2. Preliminaries

This section briefly summarizes the model analyzed and the concept of parameter varying description.

2.1. Macroscopic freeway models

In macroscopic freeway models the traffic is described by aggregated fluid-like quantities such as density $\rho(x,t)$, speed $v(x,t)$ and flow $q(x,t)$, with x being the coordinate along the freeway and t being the continuous time, but the individual vehicle dynamics are neglected.

The first-order macroscopic models are based on conservation equation (Lighthill and Whitham, 1955; Daganzo, 1994), while second-order models involve also the evolution of space-mean speed (Payne, 1971). Both equations use the partial derivative of macroscopic variables. Comparative studies emphasized the benefits of the application of second-order models. Because the real traffic phenomena are reproduced more precisely by second-order models, than by lower order ones, they are currently in the focus of problems regarding freeway control and surveillance.

An approach used widely for the numerical treatment of partial differential equations is the discretization of freeway into segments of length Δ_i, with sampling time discretization T, as illustrated in Fig. 1.

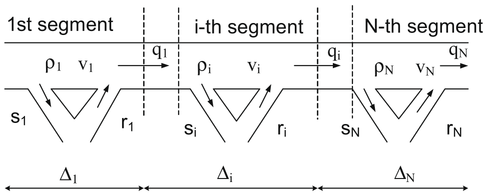

Fig. 1. Freeway division and traffic variables.

The macroscopic model was shown to work accurately with segment length up to $\Delta_i = 500–600$ m (Cremer and Papageorgiou, 1981), and the simulation time step should be chosen so that $T < \frac{\Delta_i}{v_{max}}$ holds for all segments, where v_{max} denotes the maximal possible rate of flow.

Each segment is described by its discretized traffic variables, defined as follows:

- $\rho_i(k)$ denotes the density of the ith segment at time step k $\left[\frac{\text{veh}}{\text{km}}\right]$.
- $v_i(k)$ denotes the space-mean speed of the ith segment at time step k $\left[\frac{\text{km}}{\text{h}}\right]$.
- $q_i(k)$ denotes the traffic flow leaving the ith segment at time step k $\left[\frac{\text{veh}}{\text{h}}\right]$.
- $s_i(k)$ denotes the off-ramp flow of the ith segment at time step k $\left[\frac{veh}{h}\right]$.
- $r_i(k)$ denotes the on-ramp flow of the ith segment at time step k $\left[\frac{veh}{h}\right]$.

With these notations the non-linear difference equations of the second-order macroscopic traffic flow model regarding segment i can be formulated as:

$$\rho_i(k+1) = \rho_i(k) + \frac{T}{\Delta_i n}[q_{i-1}(k) - q_i(k)] + \frac{T}{\Delta_i n}[r_i(k) - s_i(k)], \tag{1}$$

$$s_i(k) = \beta_i(k) \cdot q_{i-1}(k), \tag{2}$$

$$v_i(k+1) = v_i(k) + \frac{T}{\tau}[V(\rho_i(k)) - v_i(k)] + \frac{T}{\Delta_i} v_i(k)[v_{i-1}(k) - v_i(k)] - \frac{\nu}{\tau}\frac{T}{\Delta_i}\frac{\rho_{i+1}(k) - \rho_i(k)}{\rho_i(k) + \kappa} - \frac{\delta T}{\tau \Delta_i}\frac{r_i(k) v_i(k)}{\rho_i(k) + \kappa} + \xi_i^v(k), \tag{3}$$

$$V(\rho_i(k)) = v_f exp\left[-\frac{1}{a}\left(\frac{\rho_i(k)}{\rho_{cr}}\right)^a\right], \tag{4}$$

$$q_i(k) = \rho_i(k) \cdot v_i(k) \cdot n + \xi_i^q(k), \tag{5}$$

where n is the number of lanes and $a,\ \beta,\ v_f,\ \rho_{cr},\ \kappa,\ \tau,\ \delta,$ and ν are additional constant parameters (Papageorgiou et al., 1990). $\xi_i^v(k)$ and $\xi_i^q(k)$ are zero-mean, Gaussian system noises corrupting the speed and flow of the ith segment, respectively, at time step k. Only the deterministic case is considered in the rest of the paper. Longer sections of freeway can be built up by interconnecting several segments through the boundary variables and relations (i.e., $\rho_{i+1}(k),\ v_{i-1}(k)$).

2.2. LPV systems

An nth order deterministic discrete-time LPV model is defined as:

$$\begin{bmatrix} x(k+1) \\ y(k) \end{bmatrix} = \begin{bmatrix} A(p(k)) & B(p(k)) \\ C(p(k)) & D(p(k)) \end{bmatrix} \begin{bmatrix} x(k) \\ u(k) \end{bmatrix}, \tag{6}$$

where $x(k) \in \mathbb{R}^n$ is the state vector, $u(k) \in \mathbb{R}^{n_u}$ the input vector, $y(k) \in \mathbb{R}^{n_y}$ the output vector and $p(k) \in \mathscr{P}$ the scheduling vector in parameter variation set $\mathscr{P}$. The system is called quasi-Linear Parameter Varying (qLPV) when any of the scheduling parameters is either a state or a function of the same (Rugh and Shamma, 2000).

LPV formalism describes non-linear dynamics in a special way, by defining the scheduling parameter to capture non-linearities. That is, the dynamic evolution of the non-linearities occurring in the system may be hidden by considering them as exogenous parameters. By this way the non-linear function takes a linear-like structure. The value of an exogenous parameter needs to be known by measurements, computation or estimation (Rugh and Shamma, 2000; Wu, 1995). The entire trajectory of $p(k) \in \mathscr{P}$ is apriori not known, but the value of $p(k)$ must be available for all k time instant, and hence the system matrices $(A(p(k)),\ B(p(k)),\ C(p(k)),\ D(p(k)))$ may be reevaluated at every single time step. It is important to emphasize that scheduling parameters usually take the value from a compact set $\mathscr{P}$. Furthermore, one has to limit the number of scheduling parameters as much as possible, because the computation demands of parameter-dependent techniques rise exponentially with the dimension of the scheduling parameter.

By definition, the actual value of the parameter is required to compute the coefficients in the equation of motion. Since the selection of the scheduling parameters is not unique, the (quasi) parameter-dependent approach provides a certain modeling flexibility.

Affine parameter dependency is a special structure of the system matrices, expressed as:

$$A(p(k)) = A_0 + p_1(k)A_1 + p_2(k)A_2 + \cdots + p_m(k)A_m, \tag{7}$$

$$B(p(k)) = B_0 + p_1(k)B_1 + p_2(k)B_2 + \cdots + p_m(k)B_m, \tag{8}$$

$$C(p(k)) = C_0 + p_1(k)C_1 + p_2(k)C_2 + \cdots + p_m(k)C_m, \tag{9}$$

$$D(p(k)) = D_0 + p_1(k)D_1 + p_2(k)D_2 + \cdots + p_m(k)D_m. \tag{10}$$

Eqs. (7)–(10) express the linear dependency of coefficient matrices on the element of parameter vector p. The resulting parameter-dependent matrix is given by the linear combination of parameters $p_i,\ i = 1, \ldots, m$.

3. Derivation of qLPV model

The aim of the section is to transform non-linear freeway dynamics (1)–(5) into an LPV form (6). The transformation results in an affine quasi LPV model, which exactly covers the non-linear system. Also an approximate LPV model has been developed to reduce the computational efforts of future control and estimator designs.

3.1. Transformation techniques

Several methods (e.g., function substitution, Jacobi linearization, exact transformation) are known in the LPV literature for obtaining a parameter-dependent model (Marcos, 2001; Rugh and Shamma, 2000). The application of these techniques is restricted to some classes of non-linear functions. Methods require special properties of the structure of non-linearity, steady-state points or input-, output-mapping dimensions, in order to get an LPV description. Furthermore, the techniques are valid mainly for continuous time dynamics with ordinary differential equations. Non-linearities occurring in (1)–(5) do not satisfy the requirements above, hence these methods cannot be applied for the freeway modeling problem.

To obtain an exact solution the following integral transformation is used:

$$f(x) = F(x)x, \quad F(x) = \int_0^1 \frac{\partial f(\lambda x)}{\partial \lambda x} d\lambda, \tag{11}$$

which holds for every non-linear system that satisfies $f(0) = 0$. This transformation factorizes variable x from the non-linear continuous function $f(x)$ by co-variable λ.

At the same time, the non-linear functions in question do not satisfy the necessary condition $f(0) = 0$. To overcome this problem one has to perform a variable change in system dynamics. The basic idea is to find steady-state operation points, for which the system's dynamical evolution is zero. Then the non-linear system can be shifted into this point by introducing the new variable as the difference between the system states and steady-state point. The non-linear function is equal to zero when the new variable is zero. This variable change is called centering, described in the following sections (Isidori, 1995).

3.2. Determination of steady-states

First, steady-state values, defined as constant (i.e., not time-varying) states, should be determined for the non-linear system. The steady-state condition for discrete time systems is written as:

$$x(k+1) = x(k). \tag{12}$$

To find steady-state values one has to apply definition (12) in the state dynamics, leading to non-linear equations for the state and input variables. Variables satisfying these equations are steady-state variables, denoted by x^* and u^*. The solution can be determined by fixing one group of variables and solving the equations for the remaining ones. The selection of fixed values and conditions will characterize different steady-states. The determination of freeway steady-states are presented below.

Let us consider an interconnected chain of freeway segments where each segment may have one on-ramp and off-ramp. The speed-and density evolutions of each segment are described by Eqs. (1)–(5). Segments without off-ramp or on-ramp are the special cases of (1)–(5) with $s_i(k) = 0$ or $r_i(k) = 0$.

The steady-state values for segment $i-1$: ρ^*_{i-1} and v^*_{i-1}, are assumed to be known. The following induction method is used for determining steady-state values for downstream segments: first, substitute (2) and (5) for (1) and (4) for (3), and apply the steady-state condition (12), then the equations of the ith segment is written as:

$$\begin{aligned} 0 &= (1-\beta_i)\rho^*_{i-1}v^*_{i-1} - \rho^*_i v^*_i + r^*_i, \\ 0 &= \frac{T}{\tau}\left[V(\rho^*_i) - v^*_i\right] + \frac{T}{\Delta_i} v^*_i \left[v^*_{i-1} - v^*_i\right] - \frac{\nu}{\tau}\frac{T}{\Delta_i}\frac{\rho^*_{i+1} - \rho^*_i}{\rho^*_i + \kappa} - \frac{\delta T}{\tau \Delta_i}\frac{r^*_i v^*_i}{\rho^*_i + \kappa}. \end{aligned}$$

These equations contain four unknown variables $(\rho^*_i,\ v^*_i,\ r^*_i,\ \rho^*_{i+1})$, therefore, the solution can be obtained by fixing two of them and solving the equations for the remaining two variables. Since both density (1) and speed (3) dynamics are linear in variable $r_i(k)$, $r^*_i = 0$ is an obvious option for the steady-state value of the on-ramp volume. Another characterization of the steady-state can be done by specifying: $\rho^*_{i+1} = \rho^*_i$, i.e. vanishing anticipation term. Using these conditions, one gets:

$$\rho^*_i v^*_i = (1-\beta_i)\rho^*_{i-1}v^*_{i-1}, \tag{13}$$

$$0 = \frac{T}{\tau}\left[V(\rho^*_i) - v^*_i\right] + \frac{T}{\Delta_i} v^*_i \left[v^*_{i-1} - v^*_i\right]. \tag{14}$$

Eqs. (13) and (14) are non-linear, describing the steady-state values of the segment i. Solutions ρ^*_i and v^*_i together with the set conditions $r^*_i = 0$ and $\rho^*_i = \rho^*_{i+1}$ form the steady-state point of the section i. Naturally, the steady-state value for the density of the segment $i+1$ is also determined through the given specification. Consequently in this case an additional information is given, therefore the above used restriction $(\rho^*_{i+1} = \rho^*_i)$ is not more necessary. This implies a different solution of the steady-state problem for the segment $i+1$ as follows.

The conservation law for segment $i+1$ in this case determines the steady-state value of $v_{i+1}(k)$ (together with the selection $r^*_{i+1}=0$):

$$v^*_{i+1} = \frac{(1-\beta_{i+1})\rho^*_i v^*_i}{\rho^*_{i+1}}, \tag{15}$$

and the corresponding momentum equation can be used for determining ρ^*_{i+2}:

$$0 = \frac{T}{\tau}\left[V(\rho^*_{i+1}) - v^*_{i+1}\right] + \frac{T}{\Delta_{i+1}} v^*_{i+1}\left[v^*_i - v^*_{i+1}\right] - \frac{\nu}{\tau}\frac{T}{\Delta_i}\frac{\rho^*_{i+2}-\rho^*_{i+1}}{\rho^*_{i+1}+\kappa}. \tag{16}$$

In case of the following downstream segments, the situation of available information is always similar: known the steady-state values of the previous section and known the steady-state density for the given segment. That is to say, the construction above can be continued to determine the steady-state speed values of all downstream segments (using corresponding (15) equations) and the steady-state density values of each following segment (using the proper form of (16)).

The procedure of determining steady-state values is summarized as follows:

- Choose an operation point for the variables at the stretch origin: ρ^*_0 and v^*_0.
- Determine $\rho^*_1,\ v^*_1$ and ρ^*_2 by the help of (13) and (14) and the steady-state conditions:

$$\begin{aligned}
&r^*_1 = 0,\\
&\rho^*_2 = \rho^*_1,\\
&\rho^*_1 v^*_1 = (1-\beta_1)\rho^*_0 v^*_0,\\
&\frac{T}{\tau}\left[V(\rho^*_1) - v^*_1\right] + \frac{T}{\Delta_1} v^*_1\left[v^*_0 - v^*_1\right] = 0.
\end{aligned}$$

- Set $i=2$ and (based on (15) and (16)), perform:

$$\begin{aligned}
&r^*_i = 0\\
&v^*_i = \frac{(1-\beta_i)\rho^*_{i-1} v^*_{i-1}}{\rho^*_i},\\
&\rho^*_{i+1} = \frac{\Delta_i(\rho^*_i+\kappa)}{\nu}\left[V(\rho^*_i) - v^*_i\right] + \frac{\tau(\rho^*_i+\kappa)}{\nu} v^*_i\left[v^*_{i-1} - v^*_i\right] - \rho^*_i,\\
&i = i+1,
\end{aligned}$$

  until $i=N$.

3.3. Parameter-dependent description, exact qLPV

After the steady-state has been determined, we may shift our system by introducing the new, centered variables:

$$\begin{aligned}
&\tilde{x}(k) = x(k) - x^*,\\
&\tilde{u}(k) = u(k) - u^*.
\end{aligned}$$

Non-linear equations (1)–(5) are expressed with the new variables by substituting $x(k)=\tilde{x}(k)+x^*$ and $u(k)=\tilde{u}(k)+u^*$ for all segments. After these substitutions and rearrangement, the conservation equation for segment i is written as:

$$\begin{aligned}
\tilde{\rho}_i(k+1) = {} & \frac{T}{\Delta_i}(1-\beta_i)\left[\tilde{\rho}_{i-1}(k)\tilde{v}_{i-1}(k) + \tilde{\rho}_{i-1}(k)v^*_{i-1} + \tilde{v}_{i-1}(k)\rho^*_{i-1} - \tilde{\rho}_i(k)\tilde{v}_i(k) - \tilde{\rho}_i(k)\left(v^*_i - \frac{\Delta_i}{T}\right) - \tilde{v}_i(k)\rho^*_i\right]\\
& + \frac{T}{\Delta_i n}\tilde{r}_i(k) + \frac{T}{\Delta_i}\left[(1-\beta_i)\rho^*_{i-1}v^*_{i-1} - \rho^*_i v^*_i\right].
\end{aligned} \tag{17}$$

The last term is always zero, due to the centered condition (13), and the other terms are linear or bi-linear in the variables, therefore, these terms can be factorized without transformation. Applying the same variable change in the momentum equation, one gets:

$$\begin{aligned}
\tilde{v}_i(k+1) = {} & \tilde{v}_i(k) + \frac{T}{\tau}\left[v_f exp\left[-\frac{1}{a}\left(\frac{\tilde{\rho}_i(k)+\rho^*_i}{\rho_{cr}}\right)^a\right] - \left(\tilde{v}_i(k)+v^*_i\right)\right] + \frac{T}{\Delta_i}\left(\tilde{v}_i(k)+v^*_i\right)\left[\left(\tilde{v}_{i-1}(k)+v^*_{i-1}\right) - \left(\tilde{v}_i(k)+v^*_i\right)\right]\\
& - \frac{\nu}{\tau}\frac{T}{\Delta_i}\frac{\left(\tilde{\rho}_{i+1}(k)+\rho^*_{i+1}\right) - \left(\tilde{\rho}_i(k)+\rho^*_i\right)}{\tilde{\rho}_i(k)+\rho^*_i+\kappa} - \frac{\delta T}{n\Delta_i}\frac{\tilde{r}_i(k)\left(\tilde{v}_i(k)+v^*_i\right)}{\tilde{\rho}_i(k)+\rho^*_i+\kappa}.
\end{aligned} \tag{18}$$

Some of the terms are linear or bi-linear in the variables, therefore, can be factorized without transformation; the remaining terms are:

$$f(\tilde{\rho}_i(k),\ \tilde{v}_i(k)) = \frac{T}{\tau}\left[v_f exp\left[-\frac{1}{a}\left(\frac{\tilde{\rho}_i(k)+\rho_i^*}{\rho_{cr}}\right)^a\right] - (\tilde{v}_i(k)+v_i^*)\right] + \frac{T}{\Delta_i}v_i^*(v_{i-1}^*-v_i^*) - \frac{v}{\tau}\frac{T}{\Delta_i}\frac{\rho_{i+1}^*-\rho_i^*}{\tilde{\rho}_i(k)+\rho_i^*+\kappa}.$$

On the other hand, this function fulfils the requirement: $f(0,\ 0)=0$, due to the centering condition (14) and the definition of centered variables, therefore, variables $\tilde{\rho}_i(k)$ and $\tilde{v}_i(k)$ can be factorized out with transformation (11). The function can be divided into two parts; the first one depends on $\tilde{\rho}_i(k)$ only, while the second one on $\tilde{v}_i(k)$ only:

$$f_1(\tilde{\rho}_i(k)) = \frac{T}{\tau}\left[v_f exp\left[-\frac{1}{a}\left(\frac{\tilde{\rho}_i(k)+\rho_i^*}{\rho_{cr}}\right)^a\right] - v_i^*\right] + \frac{T}{\Delta_i}v_i^*(v_{i-1}^*-v_i^*) - \frac{v}{\tau}\frac{T}{\Delta_i}\frac{\rho_{i+1}^*-\rho_i^*}{\tilde{\rho}_i(k)+\rho_i^*+\kappa}, \tag{19}$$

$$f_2(\tilde{v}_i(k)) = \frac{T}{\tau}\tilde{v}_i(k). \tag{20}$$

The function then can be written as:

$$f(\tilde{\rho}_i(k),\ \tilde{v}_i(k)) = F_1(\tilde{\rho}_i(k))\tilde{\rho}_i(k) + F_2(\tilde{v}_i(k))\tilde{v}_i(k), \tag{21}$$

where $F_2(\tilde{v}_i(k))$ is $\frac{T}{\tau}$, obviously. The second term $F_1(\tilde{\rho}_i(k))$ is $\frac{f_1(\tilde{\rho}_i(k))}{\tilde{\rho}_i(k)}$ with a finite limit when $\tilde{\rho}_i(k)\ \rightarrow\ 0$. Since in this case both the numerator and denumerator tend to zero, the limit can be calculated by using the L'Hospital theorem, resulting in:

$$f'(0) = -\frac{exp\left(-\frac{1}{a}\left(\frac{\rho_i^*}{\rho_{cr}}\right)^a\right)\left(\frac{\rho_i^*}{\rho_{cr}}\right)^a T v_f}{\rho_i^*\tau}.$$

This means that the value of the parameter can be set to be equal with the limit.

After rearranging the terms, the momentum equation takes the following final form:

$$\begin{aligned}\tilde{v}_i(k+1) = {} & \left(\frac{T}{\Delta_i}v_i^* + \frac{T}{\Delta_i}\tilde{v}_i(k)\right)\tilde{v}_{i-1}(k) + \left(1-\frac{T}{\tau}+\frac{T}{\Delta_i}v_{i-1}^* - 2\frac{T}{\Delta_i}v_i^* - \frac{T}{\Delta_i}\tilde{v}_i(k)\right)\tilde{v}_i(k) \\ & + \left(F_1(\tilde{\rho}_i(k)) + \frac{vT}{\tau\Delta_i}\frac{1}{\tilde{\rho}_i(k)+\rho_i^*+\kappa}\right)\tilde{\rho}_i(k) - \left(\frac{vT}{\tau\Delta_i}\frac{1}{\tilde{\rho}_i(k)+\rho_i^*+\kappa}\right)\tilde{\rho}_{i+1}(k) - \frac{\delta T}{n\Delta_i}\frac{\tilde{r}_i(k)(\tilde{v}_i(k)+v_i^*)}{\tilde{\rho}_i(k)+\rho_i^*+\kappa}.\end{aligned} \tag{22}$$

Eqs. (17) and (22) can be appropriately parameterized by scheduling parameters to capture non-linearities and obtain the LPV system. The general structure is described for the case of a long freeway stretch, consisting of N segments.

The system states are chosen to be the centered density and centered space-mean speed values:

$$x(k) = [\,\tilde{\rho}_1(k) \quad \tilde{v}_i(k) \quad \cdots \quad \tilde{\rho}_i(k) \quad \tilde{v}_i(k) \quad \cdots \quad \tilde{\rho}_N(k) \quad \tilde{v}_N(k)\,].$$

The centered on-ramp values are considered as control inputs:

$$u(k) = [\,\tilde{r}_1(k) \quad \cdots \quad \tilde{r}_i(k) \quad \cdots \quad \tilde{r}_N(k)\,],$$

while the other external signals, i.e., the boundary variables are treated as measured disturbances:

$$d(k) = [\,\tilde{q}_0(k) \quad \tilde{v}_0(k) \quad \tilde{\rho}_0(k) \quad \tilde{\rho}_{N+1}(k)\,].$$

Finally, let the measured outputs be:

$$y(k) = [\,\tilde{q}_1(k) \quad \tilde{v}_1(k) \quad \tilde{q}_N(k) \quad \tilde{v}_N(k)\,].$$

The scheduling parameters for segment i are chosen to capture non-linearities in Eqs. (17) and (22):

$$p_{4i-3}(k) = \tilde{v}_i(k), \tag{23}$$

$$p_{4i-2}(k) = F_1(\tilde{\rho}_i(k)), \tag{24}$$

$$p_{4i-1}(k) = \frac{1}{\tilde{\rho}_i(k)+\rho_i^*+\kappa}, \tag{25}$$

$$p_{4i}(k) = \frac{\tilde{v}_i(k)}{\tilde{\rho}_i(k)+\rho_i^*+\kappa}. \tag{26}$$

Since these scheduling parameters are functions of the state variables, the resulting system will be a quasi-Linear Parameter Varying system in the following affine form:

$$x(k+1) = \underbrace{\left(A_0 + \sum\nolimits_{j=1}^{4N} A_j p_j(k)\right)}_{A(p(k))} x(k) + \underbrace{\left(B_0 + \sum\nolimits_{j=1}^{4N} B_j p_j(k)\right)}_{B(p(k))} u(k) + \underbrace{(\Gamma_0 + \Gamma_1 p_1(k) + \Gamma_{4N-1}p_{4N-1}(k))}_{\Gamma(p(k))} d(k). \tag{27}$$

The structure of the system matrices are given below:

$$A_0 = \begin{bmatrix} a_0^{1,1} & a_0^{1,2} & 0 & \dots & & & & & & & & & 0 \\ 0 & a_0^{2,2} & 0 & \dots & & & & & & & & & 0 \\ a_0^{3,1} & a_0^{3,2} & a_0^{3,3} & a_0^{3,4} & 0 & \dots & & & & & & & 0 \\ 0 & a_0^{4,2} & 0 & a_0^{4,4} & 0 & \dots & & & & & & & 0 \\ & & & \ddots & & & & & & & & & \vdots \\ 0 & & \dots & 0 & a_0^{2i-1,2i-3} & a_0^{2i-1,2i-2} & a_0^{2i-1,2i-1} & a_0^{2i-1,2i} & 0 & & & \dots & 0 \\ 0 & & & \dots & 0 & a_0^{2i,2i-2} & 0 & a_0^{2i,2i} & 0 & 0 & & \dots & 0 \\ & & & & & & \ddots & & & & & & \\ 0 & & & & & & \dots & 0 & a_0^{2N-1,2N-3} & a_0^{2N-1,2N-2} & & a_0^{2N-1,2N-1} & a_0^{2N-1,2N} \\ 0 & & & & & & & \dots & 0 & a_0^{2N,2N-2} & & 0 & a_0^{2N,2N} \end{bmatrix},$$

$$A_{4i-3} = \begin{bmatrix} 0 & \dots & & & & & & & \dots & 0 \\ \vdots & \ddots & & & & & & & & \vdots \\ 0 & \dots & 0 & 0 & 0 & a_{4i-3}^{2i-1,2i-1} & 0 & & \dots & 0 \\ 0 & & & 0 & a_{4i-3}^{2i,2i-2} & 0 & a_{4i-3}^{2i,2i} & 0 & \dots & 0 \\ 0 & \dots & 0 & 0 & 0 & a_{4i-3}^{2i+1,2i-1} & 0 & & \dots & 0 \\ \vdots & & & & & & & & \ddots & \vdots \\ 0 & \dots & & & & & & & \dots & 0 \end{bmatrix},$$

$$A_{4i-2} = \begin{bmatrix} 0 & \dots & & & & \dots & 0 \\ \vdots & \ddots & & & & & \vdots \\ 0 & & 0 & a_{4i-2}^{2i,2i-1} & 0 & \dots & 0 \\ \vdots & & & & & & \vdots \\ 0 & \dots & & & & \dots & 0 \end{bmatrix},$$

$$A_{4i-1} = \begin{bmatrix} 0 & \dots & & & & & & \dots & 0 \\ \vdots & \ddots & & & & & & & \vdots \\ 0 & & 0 & a_{4i-1}^{2i,2i-1} & 0 & a_{4i-1}^{2i,2i+1} & 0 & \dots & 0 \\ \vdots & & & & & & & & \vdots \\ 0 & \dots & & & & & & \dots & 0 \end{bmatrix},$$

$$A_{4i} = 0_{2N \times 2N}.$$

The non-zero entries of the parameter-dependent $A(p(k))$ matrix are collected into Table 1.
The structure and non-zero entries of the input-to-state mapping $B(p(k))$ are:

$$B_0 = \begin{bmatrix} -\frac{T}{\Delta_1 n} \\ 0 \\ -\frac{T}{\Delta_2 n} \\ \vdots \\ 0 \\ -\frac{T}{\Delta_i n} \\ 0 \\ \vdots \\ 0 \\ -\frac{T}{\Delta_N n} \\ 0 \end{bmatrix}, \quad B_{4i-1} = \begin{bmatrix} 0 \\ -\frac{\delta T}{n\Delta_1} v_1^* \\ 0 \\ \vdots \\ -\frac{\delta T}{n\Delta_i} v_i^* \\ 0 \\ -\frac{\delta T}{n\Delta_{i+1}} v_{i+1}^* \\ \vdots \\ 0 \\ -\frac{\delta T}{n\Delta_N} v_N^* \end{bmatrix}, \quad B_{4i} = \begin{bmatrix} 0 \\ -\frac{\delta T}{n\Delta_1} \\ 0 \\ \vdots \\ -\frac{\delta T}{n\Delta_i} \\ 0 \\ -\frac{\delta T}{n\Delta_{i+1}} \\ \vdots \\ 0 \\ -\frac{\delta T}{n\Delta_N} \end{bmatrix}.$$

Table 1
The non-zero entries of the parameter-independent and parameter-dependent parts of $A(p(k))$.

Parameter	Value
$a_0^{2i-1,2i-3}$	$\frac{T}{\Delta_i}(1-\beta_i)v_{i-1}^*$
$a_0^{2i-1,2i-2}$	$\frac{T}{\Delta_i}(1-\beta_i)\rho_{i-1}^*$
$a_0^{2i-1,2i-1}$	$-\frac{T}{\Delta_i}(1-\beta_i)(v_i^*-\frac{\Delta_i}{T})$
$a_0^{2i-1,2i}$	$-\frac{T}{\Delta_i}(1-\beta_i)\rho_i^*$
$a_0^{2i,2i-2}$	$\frac{T}{\Delta_i}v_i^*$
$a_0^{2i,2i}$	$1-\frac{T}{\tau}+\frac{T}{\Delta_i}v_{i-1}^*-2\frac{T}{\Delta_i}v_i^*$
$a_{4i-3}^{2i-1,2i-1}$	$-\frac{T}{\Delta_i}(1-\beta_i)$
$a_{4i-3}^{2i,2i}$	$-\frac{T}{\Delta_i}$
$a_{4i-3}^{2i,2i-2}$	$\frac{T}{\Delta_i}$
$a_{4i-3}^{2i+1,2i-1}$	$\frac{T}{\Delta_{i+1}}(1-\beta_{i+1})$
$a_{4i-2}^{2i,2i-1}$	1
$a_{4i-1}^{2i,2i-1}$	$\frac{\nu T}{\tau\Delta_i}$
$a_{4i-1}^{2i,2i+1}$	$-\frac{\nu T}{\tau\Delta_i}$

Table 2
The non-zero entries of parameter-independent and parameter-dependent parts of $C(p(k))$.

Parameter	Value
$c_0^{1,1}$	1
$c_0^{3,2N-1}$	1
$c_1^{2,2}$	n
$c_{4N-1}^{4,2N}$	n

The direction of the measured disturbances is given with $\Gamma(p(k))$:

$$\Gamma_0=\begin{bmatrix}\frac{T}{\Delta_1} & \frac{T}{\Delta_1}\rho_1^* & \frac{T}{\Delta_1}v_1^* & 0\\ 0 & \frac{T}{\Delta_1}v_1^* & 0 & 0\\ \vdots & \vdots & \vdots & \vdots\\ 0 & 0 & 0 & 0\end{bmatrix},\quad \Gamma_1=\begin{bmatrix}0 & 0 & 0 & 0\\ 0 & \frac{T}{\Delta_1} & 0 & 0\\ 0 & 0 & 0 & 0\\ \vdots & \vdots & \vdots & \vdots\\ 0 & 0 & 0 & 0\end{bmatrix},\quad \Gamma_{4N-1}=\begin{bmatrix}0 & 0 & 0 & 0\\ \vdots & \vdots & \vdots & \vdots\\ 0 & 0 & 0 & 0\\ 0 & 0 & 0 & -\frac{\nu T}{\Delta_N n}\end{bmatrix}.$$

The measurement equation of the system can be written as:

$$y(k)=(C_0+C_1p_1(k)+C_{4N-3}p_{4N-3}(k))x(k), \tag{28}$$

where the non-zero elements of the parameter-dependent $C(p(k))$ is summarized in Table 2.

During the derivation of the LPV model no approximations were made, the resulting system is equivalent with the non-linear model, i.e., covers the same system. One may also notice that this description uses four scheduling parameters (23)–(26) for one segment with two state variables. Since the computational demands of parameter-dependent design methods (identification, estimator and controller design) increase exponentially with the dimension of the scheduling parameter vector, this parametrization implies heavy off-line computations. A reasonable way to reduce these computational needs is the approximation of some non-linear terms instead of treating them as scheduling parameters.

3.4. Approximate qLPV description

Since two scheduling parameters, ($p_{4i-1}(k)$ in (25) and $p_{4i}(k)$ in (26)) depend on term $(\tilde{\rho}_i(k)+\rho_i^*+\kappa)^{-1}$, an approximation of this term would significantly decrease the computational efforts. The approximation can be done by replacing the term with a constant one (denoted with: κ^+) and determine the steady-state values according to this new dynamics. The steady-state equations take a similar form as previously introduced (3.2). The only difference is in terms containing the modified dynamics, i.e., the anticipation term and the term expressing the speed decreasing effect of on-ramps are modified.

Let us denote the steady-state values of the ith segment, regarding the modified dynamics, by ρ_i^+ and v_i^+. Introducing the new variables as the difference between state variables and steady-states (Section 3.3), rearranging terms and applying factorization (11), one gets as follows:

$$\tilde{\rho}_i(k+1) = \frac{T}{\Delta_i}(1-\beta_i)\left[\tilde{\rho}_{i-1}(k)\tilde{v}_{i-1}(k) + \tilde{\rho}_{i-1}(k)v^+_{i-1} + \tilde{v}_{i-1}(k)\rho^+_{i-1} - \tilde{\rho}_i(k)\tilde{v}_i(k) + \tilde{\rho}_i(k)\left(v^+_i - \frac{\Delta_i}{T}\right) - \tilde{v}_i(k)\rho^+_i\right] + \frac{T}{\Delta_i n}\tilde{r}_i(k) + \frac{T}{\Delta_i}\left[(1-\beta_i)\rho^+_{i-1}v^+_{i-1} - \rho^+_i v^+_i\right], \tag{29}$$

$$\tilde{v}_i(k+1) = \left(\frac{T}{\Delta_i}v^+_i + \frac{T}{\Delta_i}\tilde{v}_i(k)\right)\tilde{v}_{i-1}(k) + \left(1 - \frac{T}{\tau} + \frac{T}{\Delta_i}v^+_{i-1} - 2\frac{T}{\Delta_i}v^+_i - \frac{T}{\Delta_i}\tilde{v}_i(k)\right)\tilde{v}_i(k) + \left(F^+_1(\tilde{\rho}_i(k)) + \frac{\nu T}{\tau\Delta_i}\frac{1}{\kappa^+}\right)\tilde{\rho}_i(k) - \left(\frac{\nu T}{\tau\Delta_i}\frac{1}{\kappa^+}\right)\tilde{\rho}_{i+1}(k) - \frac{\delta T}{n\Delta_i}\frac{\tilde{r}_i(k)\left(\tilde{v}_i(k)+v^+_i\right)}{\kappa^+}, \tag{30}$$

where $F^+_1(\tilde{\rho}_i(k))$ denotes the result of the transformation from non-linear function $f^+_1(\tilde{\rho}_i(k))$:

$$f^+_1(\tilde{\rho}_i(k)) = \frac{T}{\tau}\left[v_f exp\left[-\frac{1}{a}\left(\frac{\tilde{\rho}_i(k)+\rho^+_i}{\rho_{cr}}\right)^a\right] - v^+_i\right] + \frac{T}{\Delta_i}v^+_i(v^+_{i-1} - v^+_i) - \frac{\nu}{\tau}\frac{T}{\Delta_i}\frac{\rho^+_{i+1}-\rho^+_i}{\kappa^+}. \tag{31}$$

To capture non-linearities in Eqs. (29) and (30) it is sufficient to introduce only two scheduling parameters as follows:

$$p^+_{2i-1}(k) = \tilde{v}_i(k), \tag{32}$$
$$p^+_{2i}(k) = F^+_1(\tilde{\rho}_i(k)). \tag{33}$$

The resulting system is a quasi-Linear Parameter Varying system with affine parameter-dependent system matrices:

$$x(k+1) = \underbrace{\left(A^+_0 + \sum_{j=1}^{2N} A^+_j p^+_j(k)\right)}_{A^+(p^+(k))} x(k) + \underbrace{\left(B^+_0 + \sum_{j=1}^{2N} B^+_j p^+_j(k)\right)}_{B^+(p^+(k))} u(k) + \underbrace{\left(\Gamma^+_0 + \Gamma^+_1 p^+_1(k)\right)}_{\Gamma^+(p^+(k))} d(k). \tag{34}$$

The structure of the system matrices is given below:

$$A^+_0 = \begin{bmatrix}
a_0^{1,1} & a_0^{1,2} & 0 & \dots & & & & & & & & 0\\
a_0^{2,1} & a_0^{2,2} & a_0^{2,3} & \dots & & & & & & & & 0\\
a_0^{3,1} & a_0^{3,2} & a_0^{3,3} & a_0^{3,4} & 0 & \dots & & & & & & 0\\
0 & a_0^{4,2} & a_0^{4,3} & a_0^{4,4} & a_0^{4,5} & \dots & & & & & & 0\\
 & & & \ddots & & & & & & & & \vdots\\
0 & & \dots & 0 & a_0^{2i-1,2i-3} & a_0^{2i-1,2i-2} & a_0^{2i-1,2i-1} & a_0^{2i-1,2i} & 0 & & \dots & 0\\
0 & & & \dots & 0 & a_0^{2i,2i-2} & a_0^{2i,2i-1} & a_0^{2i,2i} & a_0^{2i,2i+1} & 0 & \dots & 0\\
 & & & & & & \ddots & & & & & \\
0 & & & & & & \dots & 0 & a_0^{2N-1,2N-3} & a_0^{2N-1,2N-2} & a_0^{2N-1,2N-1} & a_0^{2N-1,2N}\\
0 & & & & & & & \dots & 0 & a_0^{2N,2N-2} & 0 & a_0^{2N,2N}
\end{bmatrix},$$

$$A^+_{2i-1} = \begin{bmatrix}
0 & \dots & & & & & & \dots & 0\\
\vdots & \ddots & & & & & & & \vdots\\
0 & \dots & 0 & 0 & 0 & a_{2i-1}^{2i-1,2i-1} & 0 & \dots & 0\\
0 & & & 0 & a_{2i-1}^{2i,2i-2} & 0 & a_{2i-1}^{2i,2i} & 0\ \dots & 0\\
0 & \dots & 0 & 0 & 0 & a_{2i-1}^{2i+1,2i-1} & 0 & \dots & 0\\
\vdots & & & & & & & \ddots & \vdots\\
0 & \dots & & & & & & \dots & 0
\end{bmatrix},$$

$$A^+_{2i} = \begin{bmatrix}
0 & \dots & & & & \dots & 0\\
\vdots & \ddots & & & & & \vdots\\
0 & & 0 & a_{2i}^{2i,2i-1} & 0 & \dots & 0\\
\vdots & & & & & & \vdots\\
0 & \dots & & & & \dots & 0
\end{bmatrix}.$$

Table 3
The non-zero entries of the parameter-independent and parameter-dependent parts of $A^+(p^+(k))$.

Parameter	Value
$a_0^{2i-1,2i-3}$	$\frac{T}{\Delta_i}(1-\beta_i)v_{i-1}^+$
$a_0^{2i-1,2i-2}$	$\frac{T}{\Delta_i}(1-\beta_i)\rho_{i-1}^+$
$a_0^{2i-1,2i-1}$	$\frac{T}{\Delta_i}(1-\beta_i)(v_i^+ - \frac{\Delta_i}{T})$
$a_0^{2i-1,2i}$	$-\frac{T}{\Delta_i}(1-\beta_i)\rho_i^+$
$a_0^{2i,2i-1}$	$\frac{\nu T}{\tau \Delta_i}\frac{1}{\kappa^+}$
$a_0^{2i,2i-2}$	$\frac{T}{\Delta_i}v_i^+$
$a_0^{2i,2i}$	$1-\frac{T}{\tau}+\frac{T}{\Delta_i}v_{i-1}^+ - 2\frac{T}{\Delta_i}v_i^+$
$a_0^{2i,2i+1}$	$-\frac{\nu T}{\tau \Delta_i}\frac{1}{\kappa^+}$
$a_{2i-1}^{2i-1,2i-1}$	$-\frac{T}{\Delta_i}(1-\beta_i)$
$a_{2i-1}^{2i,2i}$	$-\frac{T}{\Delta_i}$
$a_{2i-1}^{2i,2i-2}$	$\frac{T}{\Delta_i}$
$a_{2i-1}^{2i+1,2i-1}$	$\frac{T}{\Delta_{i+1}}(1-\beta_{i+1})$
$a_{2i}^{2i,2i-1}$	1

The non-zero entries of parameter-dependent matrix $A^+(p^+(k))$ are collected into Table 3.

The structure and non-zero entries of input-to-state mapping $B^+(p^+(k))$ are:

$$B_0^+ = \begin{bmatrix} -\frac{T}{\Delta_1 n} \\ -\frac{\delta T}{n\Delta_1}\frac{v_1^+}{\kappa^+} \\ -\frac{T}{\Delta_2 n} \\ -\frac{\delta T}{n\Delta_2}\frac{v_2^+}{\kappa^+} \\ \vdots \\ -\frac{T}{\Delta_i n} \\ -\frac{\delta T}{n\Delta_i}\frac{v_i^+}{\kappa^+} \\ -\frac{T}{\Delta_{i+1} n} \\ -\frac{\delta T}{n\Delta_{i+1}}\frac{v_i^+}{\kappa^+} \\ \vdots \\ -\frac{T}{\Delta_N n} \\ -\frac{\delta T}{n\Delta_N}\frac{v_N^+}{\kappa^+} \end{bmatrix}, \quad B_{2i-1}^+ = \begin{bmatrix} 0 \\ -\frac{\delta T}{n\Delta_1}v_1^+ \\ 0 \\ \vdots \\ -\frac{\delta T}{n\Delta_i}v_i^+ \\ 0 \\ -\frac{\delta T}{n\Delta_{i+1}}v_{i+1}^+ \\ \vdots \\ 0 \\ -\frac{\delta T}{n\Delta_N}v_N^+ \end{bmatrix}.$$

The measured disturbances act on the state evolution specified by $\Gamma^+(p_1^+(k))$:

$$\Gamma_0^+ = \begin{bmatrix} \frac{T}{\Delta_1} & \frac{T}{\Delta_1}\rho_1^+ & \frac{T}{\Delta_1}v_1^+ & 0 \\ 0 & \frac{T}{\Delta_1}v_1^+ & 0 & 0 \\ \vdots & \vdots & \vdots & \vdots \\ 0 & 0 & 0 & -\frac{\nu T}{\Delta_N n}v_N^+ \end{bmatrix}, \quad \Gamma_1^+ = \begin{bmatrix} 0 & 0 & 0 & 0 \\ 0 & \frac{T}{\Delta_1} & 0 & 0 \\ 0 & 0 & 0 & 0 \\ \vdots & \vdots & \vdots & \vdots \\ 0 & 0 & 0 & 0 \end{bmatrix}.$$

One has to emphasize that the neglected dynamics caused by the approximation introduced in this section, together with other modeling simplifications, can be taken into account through robust LPV controller design.

4. Numerical example

The presented qLPV freeway models have been investigated through simulations, using real detector measurement data. These simulations validate the tracking capability of models under varying traffic conditions.

4.1. Test field and simulation setup

A 3.5 km long stretch of freeway A12 in the Netherlands has been used as a test field to validate the qLPV model. The schematic road topology can be seen in Fig. 2.

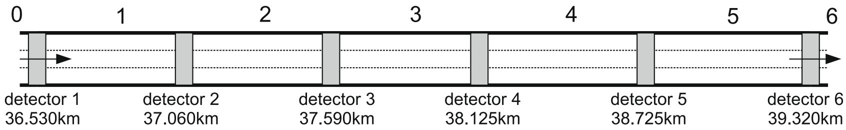

Fig. 2. The schematic road topology and detector spacing of the test field.

Six detector stations are located in this stretch, registering the traffic flow and time-mean speed values with a sample time of 60 s. Due to the lack of actual speed values of individual vehicles, the measured time-mean speed is treated as space-mean speed and is used during simulations. Traffic density was calculated by using the fundamental relationship between traffic variables (Eq. (5)). The stretch has been subdivided into five segments according to the detector locations. The lengths of the segments are as follows:

$$\Delta = [530\ 530\ 535\ 600\ 595]\ \text{m}.$$

For simulation purposes the detector measurement data have been re-sampled with $T = 10$ s, using linear interpolation between the originally measured values. In order to investigate the power of qLPV traffic model, a traffic scenario has been chosen, which contains both free-and interrupted flow cases. The data were collected on 23.01.2006 between 6.00 AM and 11.00 AM. The traffic conditions in time and space are illustrated by speed values in Fig. 3.

The diagram clearly shows two traffic breakdowns propagating through the stretch during the observation period.

4.2. Non-linear model identification and validation

In order to calculate the scheduling parameters and the parameter-dependent system matrices of the qLPV model, one has to know the unknown parameters of the non-linear model. To determine these model parameters, the optimization method proposed by Cremer and Papageorgiou (1981) has been performed by using different data sets containing various traffic situations. For each data set the algorithm has been initialized from a number of starting points in order to avoid local optima. The results are summarized in Table 4.

In order to obtain the best approximate qLPV model, a non-linear term has been replaced by a constant one (Section 3.4) and the identification procedure has been repeated to determine the parameters of this modified dynamics. In this case the optimal parameters are collected in Table 5.

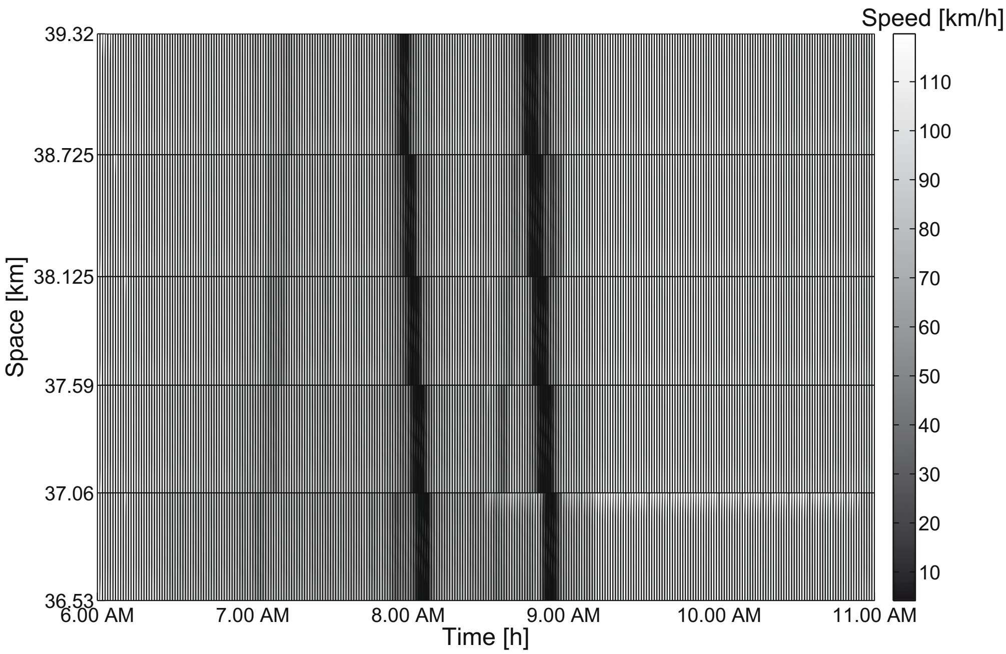

Fig. 3. Time–space diagram of the chosen traffic situation for simulation.

Table 4
The identified parameters of the non-linear model.

τ [h]	v_{free} $\left[\frac{\text{km}}{\text{h}}\right]$	a_m	κ $\left[\frac{\text{veh}}{\text{kmlane}}\right]$	ν $\left[\frac{\text{km}^2}{\text{h}}\right]$	ρ_{cr} $\left[\frac{\text{veh}}{\text{kmlane}}\right]$
0.0039	113.0517	3.7619	3.5963	33.7698	23.4246

Table 5
The identified parameters of the approximate non-linear model.

τ [h]	v_{free} $\left[\frac{\text{km}}{\text{h}}\right]$	a_m	κ^+ $\left[\frac{\text{veh}}{\text{kmlane}}\right]$	ν $\left[\frac{\text{km}^2}{\text{h}}\right]$	ρ_{cr} $\left[\frac{\text{veh}}{\text{kmlane}}\right]$
0.0087	116.4057	4.3982	20.7729	29.3505	22.5324

4.3. Exact qLPV model description and validation

Once the unknown parameters are determined, we are able to calculate the steady-state values of the exact model, according to (13)–(16). The test-field segments are considered as the special case of these equations without off-ramp and on-ramp. The construction result in the same steady-state value for each segment:

$$\rho^* = 23.4246\ \frac{\text{veh}}{\text{km lane}},$$
$$v^* = 86.6629\ \frac{\text{km}}{\text{h}}.$$

With the above information, together with Table 4 the parameter-dependent matrices can be computed by Section 3.3. The segmentation of the stretch implies a ten-dimensional state-space, hence the $A(p)$ matrices are 10×10 dimensional. The components of $A(p)$ are as follows:

$$A_0 = \begin{bmatrix} 0.5458 & -0.1228 & 0 & 0 & 0 & 0 & 0 & 0 & 0 & 0 \\ 0 & -0.1667 & 0 & 0 & 0 & 0 & 0 & 0 & 0 & 0 \\ 0.4542 & 0.1228 & 0.5458 & -0.1228 & 0 & 0 & 0 & 0 & 0 & 0 \\ 0 & 0.4542 & 0 & -0.1667 & 0 & 0 & 0 & 0 & 0 & 0 \\ 0 & 0 & 0.4500 & 0.1216 & 0.5500 & -0.1216 & 0 & 0 & 0 & 0 \\ 0 & 0 & 0 & 0.4500 & 0 & -0.1624 & 0 & 0 & 0 & 0 \\ 0 & 0 & 0 & 0 & 0.4012 & 0.1084 & 0.5988 & -0.1084 & 0 & 0 \\ 0 & 0 & 0 & 0 & 0 & 0.4012 & 0 & -0.1137 & 0 & 0 \\ 0 & 0 & 0 & 0 & 0 & 0 & 0.4046 & 0.1094 & 0.5954 & -0.1094 \\ 0 & 0 & 0 & 0 & 0 & 0 & 0 & 0.4046 & 0 & -0.1171 \end{bmatrix}$$

The elements of A_{4i-3}, $i = 1, \ldots, 5$ are determined by $\frac{T}{\Delta_i}$, these values are collected in Table 6 and the matrix structures are given in Section 3.3.

The non-zero entries of A_{4i-1}, $i = 1, \ldots 5$ are determined by $\frac{\nu T}{\tau \Delta_i}$, which takes the following values in case of the different segments (see Table 7), and the matrix structures are given in Section 3.3.

Since the system contains no on-ramps, the parameter-dependent $B(p)$ is not necessary. The direction of the measured disturbances $\tilde{\rho}_0$, $\tilde{v}_0$, $\tilde{q}_0$, $\tilde{\rho}_6$ is constructed according to Section 3.3. The numerical values needed for $\Gamma(p)$ are summarized in Table 8.

Table 6
The numerical values of the non-zero entries in A_{4i-3}, $i = 1, \ldots, 5$.

$i = 1$	$i = 2$	$i = 3$	$i = 4$	$i = 5$
0.0052	0.0052	0.0052	0.0046	0.0047

Table 7
The numerical values of the non-zero entries in A_{4i-1}, $i = 1, \ldots, 5$.

$i = 1$	$i = 2$	$i = 3$	$i = 4$	$i = 5$
45.3970	45.3970	44.9727	40.1006	40.4376

Table 8
The numerical values of the non-zero entries in $\Gamma(p)$.

$\frac{T}{\Delta_1}$	$\frac{T}{\Delta_1}\rho_1^*$	$\frac{T}{\Delta_1}v_1^*$	$-\frac{\nu T}{\tau\Delta_5}$
0.0052	0.1228	0.4542	−40.4376

After the parameter-dependent system matrices are determined, it is possible to investigate its behavior by using real detector measurement data introduced in Section 4.1. During the simulation the measurements of detector 1 and detector 6 were centered according to the definition of centered variables and used as input. The steady-state values are subtracted from these measurements and then $\tilde{\rho}_0,\ \tilde{v}_0,\ \tilde{q}_0,\ \tilde{\rho}_6$ excited the parameter-dependent dynamics. The density and speed responses of the qLPV model are compared with the measured values of detector 4. Comparative plots are given in Figs. 4 and 5.

4.4. Approximate qLPV model description and validation

The approximate qLPV model has been set up for investigating its accuracy and the effect of simplifications involved in Section 3.4. The steady-state for segments, now, takes the following values:

$$\rho^+ = 24.7228\ \frac{\text{veh}}{\text{km lane}},$$
$$v^+ = 93.1674\ \frac{\text{km}}{\text{h}}.$$

With the above information, together with the identified parameters of the approximate non-linear dynamics in Table 5, the parameter-dependent matrices can be computed by Section 3.4. The components of $A^+(p^+(k))$ are as follows:

$$A_0^+ = \begin{bmatrix} 0.5117 & -0.1176 & 0 & 0 & 0 & 0 & 0 & 0 & 0 & 0 \\ 17.5686 & 0.1924 & -17.5686 & 0 & 0 & 0 & 0 & 0 & 0 & 0 \\ 0.4883 & 0.1176 & 0.5117 & -0.1176 & 0 & 0 & 0 & 0 & 0 & 0 \\ 0 & 0.4883 & 17.5686 & 0.1924 & -17.5686 & 0 & 0 & 0 & 0 & 0 \\ 0 & 0 & 0.4837 & 0.1165 & 0.5163 & -0.1165 & 0 & 0 & 0 & 0 \\ 0 & 0 & 0 & 0.4837 & 17.4044 & 0.1970 & -17.4044 & 0 & 0 & 0 \\ 0 & 0 & 0 & 0 & 0.4313 & 0.1039 & 0.5687 & -0.1039 & 0 & 0 \\ 0 & 0 & 0 & 0 & 0 & 0.4313 & 15.5189 & 0.2494 & -15.5189 & 0 \\ 0 & 0 & 0 & 0 & 0 & 0 & 0.4350 & 0.1048 & 0.5650 & -0.1048 \\ 0 & 0 & 0 & 0 & 0 & 0 & 0 & 0.4350 & 15.6493 & 0.2458 \end{bmatrix}$$

The elements of $A_{2i},\ i = 1,\dots,5$ are determined by $\frac{T}{\Delta_i}$, collected in Table 6 and the matrix structures are described in Section 3.4.

Since the system contains no on-ramps, the parameter-dependent $B^+(p^+)(k)$ is not necessary. The direction of the measured disturbances $\tilde{\rho}_0,\ \tilde{v}_0,\ \tilde{q}_0, \tilde{\rho}_6$ is constructed as in Section 3.4. The numerical values needed for $\Gamma^+(p^+(k))$ are summarized in Table 9.

The simulation of the approximate qLPV model was performed using the same exciting data sets. The density and speed responses of the approximate qLPV model were compared with the measured values of detector 4. Comparative plots are given in Figs. 6 and 7.

4.5. Evaluation of the results

During the derivation of the exact qLPV model no approximations are introduced, i.e., the obtained parameter-dependent traffic model gives the same response as the non-linear one. Also the simulation experience verifies, i.e., the relative differences between the responses of the different representations were of the magnitude of 10^{-4}. The difference is originated in the alternative numerical computational techniques. Figs. 4 and 5 clearly illustrate that the qLPV description produces the same tracking capability and accuracy as the non-linear one and is able to reproduce traffic phenomena. This means that the obtained model description preserves the non-linear dynamics of traffic flow in a compact and very attractive linear like form.

The effects of the approximation on the model fitting can be seen in Fig. 6. A degradation of the approximated description is originated from neglecting non-linearities in the anticipation term. One can see oscillation in the speed response under rapidly varying traffic conditions, around 8 AM and before 9 AM. Fig. 7 shows one traffic breakdown more into the details in order to observe these oscillations caused by the neglected dynamics. Moreover, the approximated dynamics give sharp responses for traffic breakdowns, due to the modified parameter set. The new set of parameters results in a relatively slow,

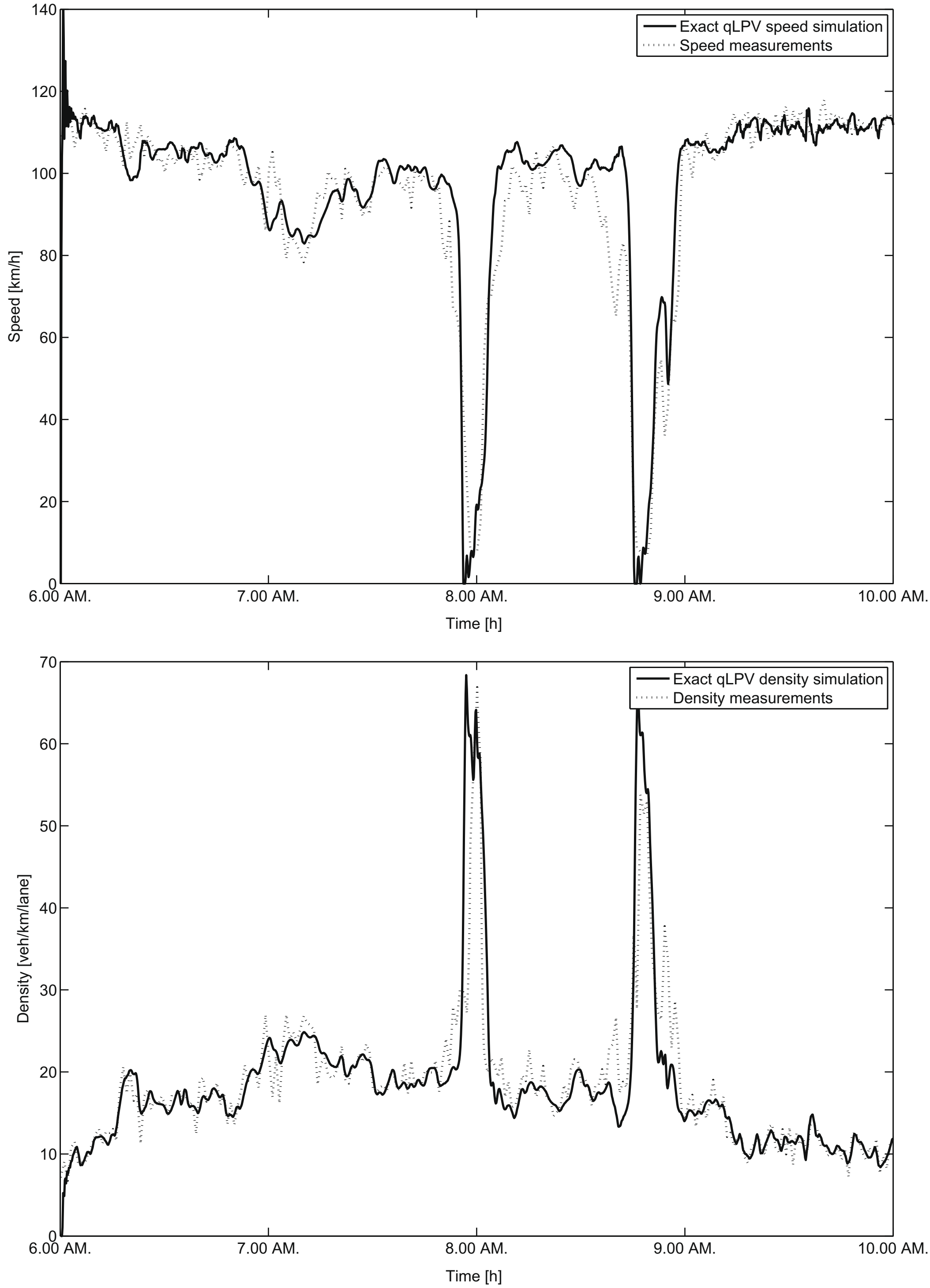

Fig. 4. Comparison of exact qLPV speed and density responses with detector measurement data.

delayed model reaction with narrow transients. This phenomena can be seen in the density response in Fig. 7 the most. As one may conclude, the accuracy of the model has been reduced in two different ways when traffic conditions change suddenly, respectively as a consequence of the neglected dynamics. At the same time, the approximated qLPV model is also able to reproduce traffic phenomena, but with a lower accuracy.

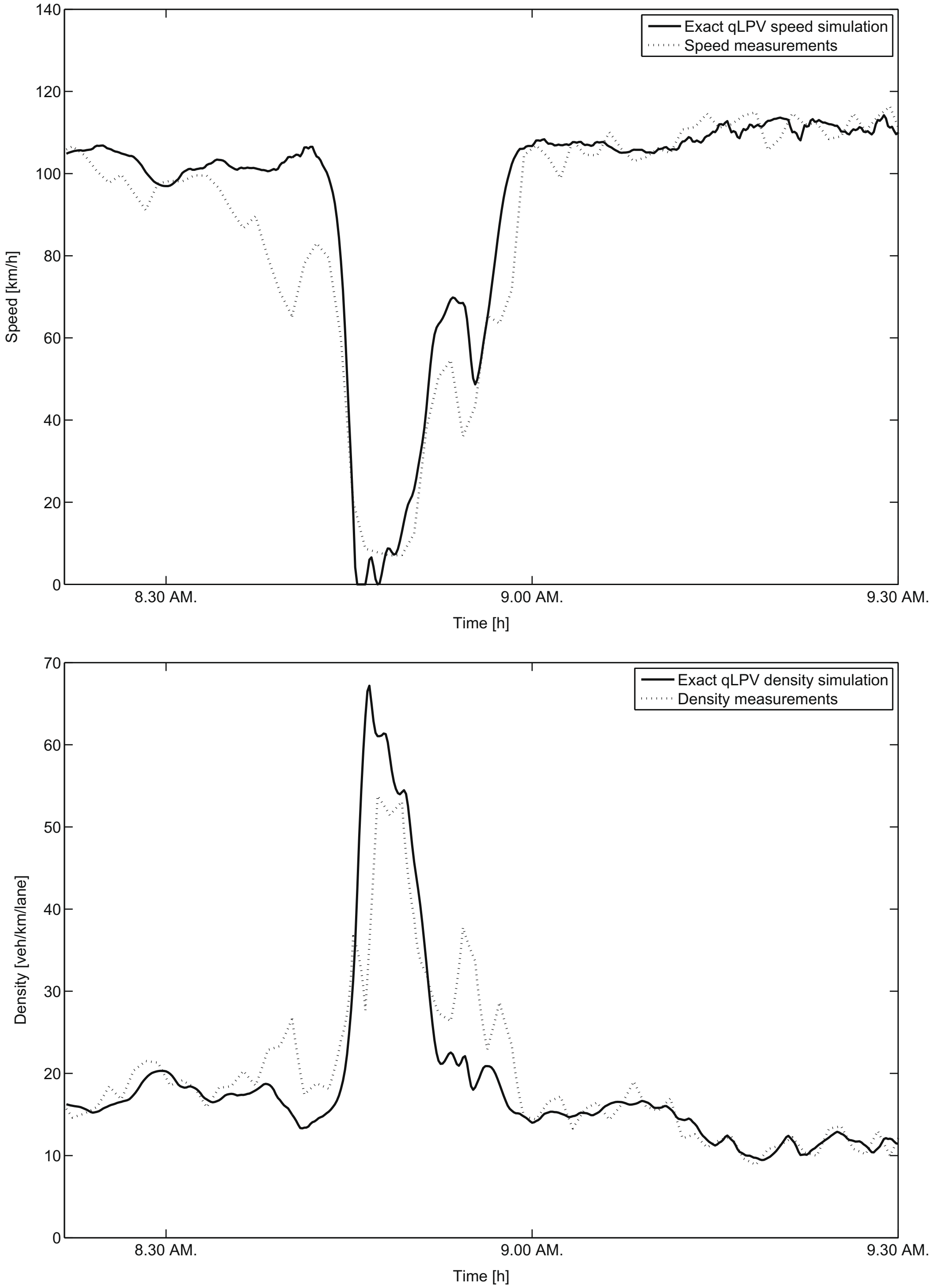

Fig. 5. Tightened view of exact qLPV speed and density responses with detector measurement data under a traffic breakdown.

Table 9
The numerical values of the non-zero entries in $\Gamma^{+}(p^{+}(k))$.

$\frac{T}{\Delta_1}$	$\frac{T}{\Delta_1}\rho^{+}$	$\frac{T}{\Delta_1}v^{+}$	v^{+}	$-\frac{\nu T}{\tau\Delta_5}$
0.0052	0.1176	0.4883	93.1674	−15.6493

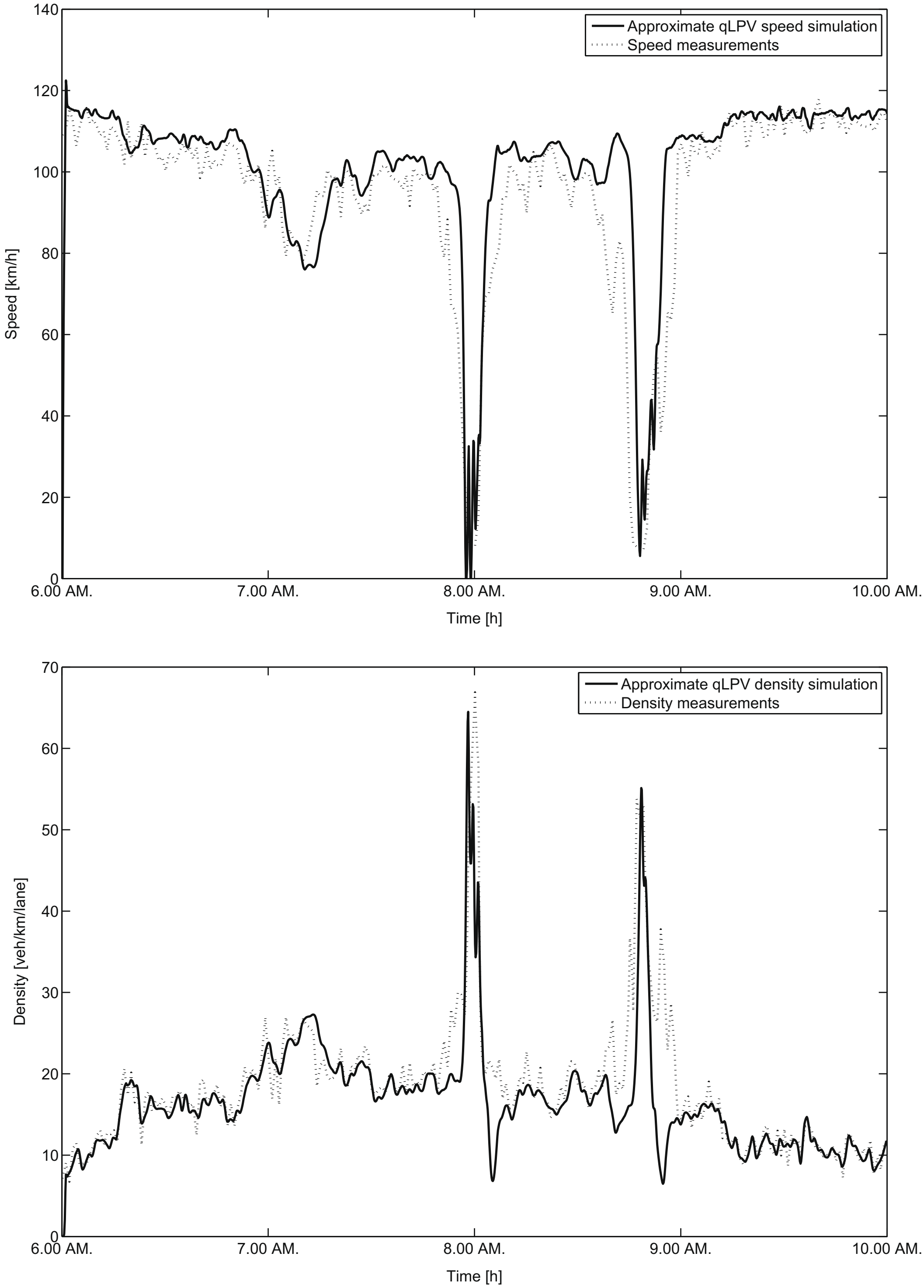

Fig. 6. Comparison of approximate qLPV speed and density responses with detector measurement data.

In order to compare the two models, the Variation Accounted For (VAF) is calculated in both cases. The VAF is defined as follows:

$$\mathrm{VAF}(y(k),\ \hat{y}(k)) = 100 \times max\left\{1 - \frac{\mathrm{var}(y(k) - \hat{y}(k))}{\mathrm{var}(y(k))},\ 0\right\}, \tag{35}$$

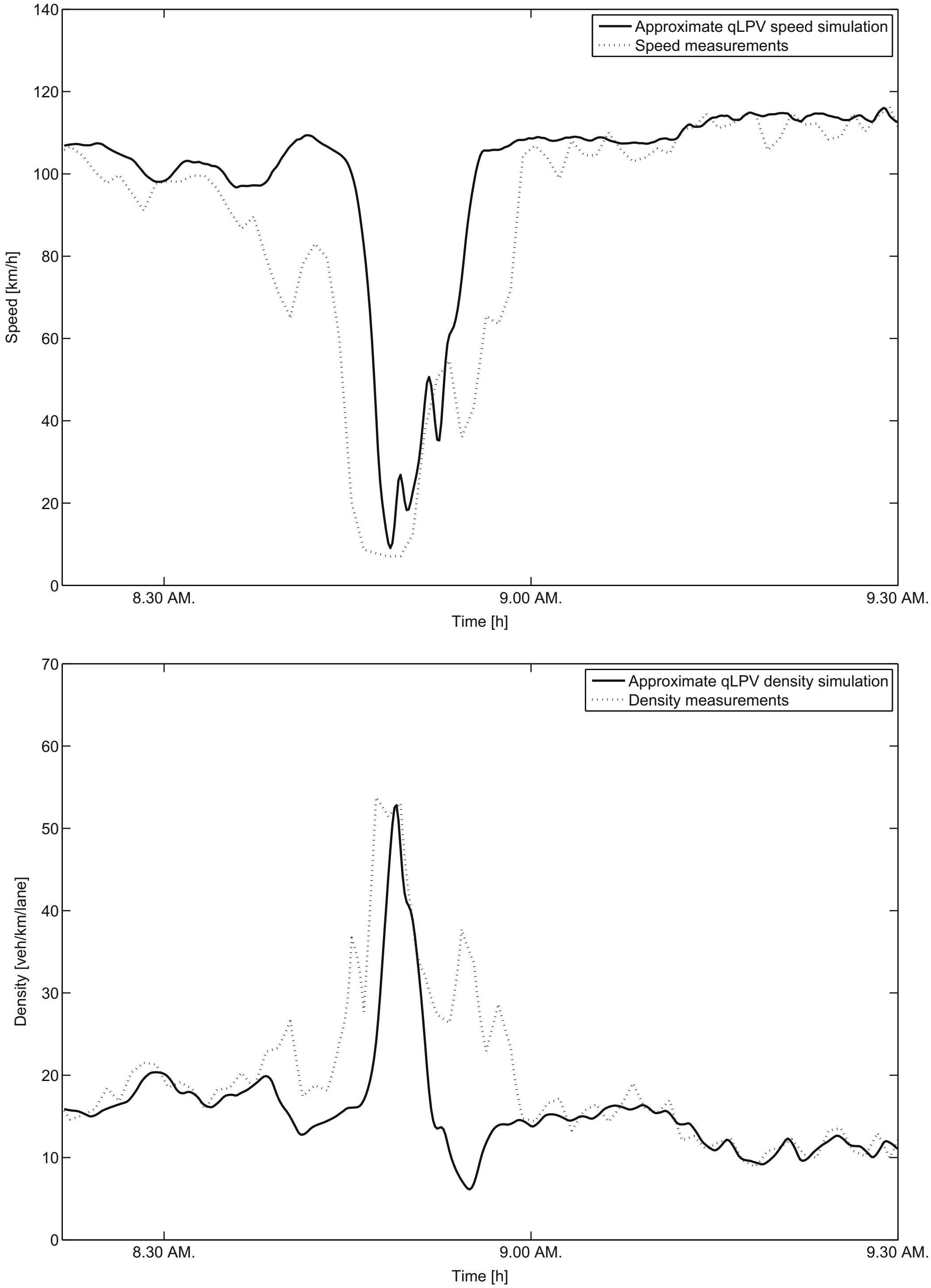

Fig. 7. Tightened view of approximate qLPV speed and density responses with detector measurement data under a traffic breakdown.

where $y(k)$ denotes the real measured outputs, while $\hat{y}(k)$ is the simulated output of the identified model. The function $var(\cdot)$ refers to the variance of the quasi-stationary signals. The VAF values for the exact qLPV model are:

$$\mathrm{VAF}_{\rho}^{\mathrm{ex}} = 71.53,$$
$$\mathrm{VAF}_{v}^{\mathrm{ex}} = 86.08,$$

while in the approximated case:

$$\mathrm{VAF}_{\rho}^{\mathrm{ap}} = 68.8,$$
$$\mathrm{VAF}_{v}^{\mathrm{ap}} = 72.96.$$

The VAF clearly shows the differences between the exact and approximated qLPV models. The approximation causes a 15% decrease in the accuracy of the speed and due to this mismatch a 4% difference in the density evolution.

These mismatches between real measurements and model responses can be handled by introducing model uncertainties. One can easily characterize the difference between real and simulated signals and take these information into consideration through the robust controller design procedure. Robust controller design techniques are summarized in the LPV literature (Wu, 1995). One can design controllers which are proved to robustly stabilize the real system using the nominal mathematical model and the information of neglected dynamics. Systematic robust control synthesis for non-linear systems is still an open problem in systems and control theory. Hence the introduced qLPV reformulation may serve to design parameter-dependent and robust controllers for freeway traffic.

5. Conclusion and further research

The paper presents the Linear Parameter Varying (LPV) formulation of a generic freeway traffic model. The derivation of the quasi LPV (qLPV) structure with affine parameter dependency is proposed for identification, control, estimation and diagnosis.

The exact reformulation of the non-linear traffic model to qLPV system requires non-conventional approaches, due to the discrete nature of the macroscopic description and the non-centered non-linearity in the second order moment term. Therefore, the paper introduces a generic centering process of the state variables and uses an integral transformation to factorize the same variable from non-linearity, resulting in an qLPV model. Two different parameter-dependent models are presented. First, the exact qLPV reformulation of the non-linear system is defined by using a relatively high number of parameters per freeway section. Afterwards, a possible and reasonable simplification in the parameter vector allows us to create an approximate qLPV model by neglecting some of the dynamics.

Real traffic measurement based model validation illustrates the viability of the method suggested.

Further research will focus on applying of the parameter-dependent estimation and control theory (i.e., robust model predictive and induced $\mathscr{L}_2$ norm control, estimation) aiming at freeway surveillance.

Acknowledgments

The traffic data are provided by, and used with the permission of Rijkswaterstaat-Centre for Transport and Navigation. The authors express their thanks to Andras Hegyi from Delft University of Technology, Faculty of Civil Engineering, for his valuable and important comments. The authors gratefully acknowledge to the support by the Hungarian National Scientific Research Fund (OTKA CNK78168).

References

Cremer, M., Papageorgiou, M., 1981. Parameter identification for a traffic flow model. Automatica 17 (6), 837–843.

Daganzo, C.F., 1994. The cell transmission model: a dynamic representation of highway traffic consistent with the hydrodynamic theory. Transportation Research Part B 28B (4), 269–287.

Daganzo, C.F., 1995. Requiem for second-order fluid approximations of traffic flow. Transportation Research Part B 29 (4), 277–286.

Hangos, K., Bokor, J., Szederkényi, G., 2004. Analysis and Control of Nonlinear Process Systems. Springer.

Hegyi, A., Schutter, B.D., Hellendoorn, H., 2005. Model predictive control for optimal coordination of ramp metering and variable speed limits. Transportation Research Part C 13 (3), 185–209.

Hoogendoorn, S., Bovy, P., 2001. State-of-the-art of vehicular traffic flow modelling. Proceedings of the Institution of Mechanical Engineers, Part I. Systems and Control Engineering 215 (14), 283–303.

Isidori, A., 1995. Nonlinear Control Systems. Springer Verlag.

Leutzbach, W., 1988. An Introduction to the Theory of Traffic Flow. Springer Verlag, Berlin.

Lighthill, M., Whitham, G., 1955. On kinematic waves. Part I: flood movement in long rivers. Part II. A theory of traffic flow on long crowded roads. Proceedings Royal Society A229, 281–345.

Marcos, A., 2001. A Linear Parameter Varying Model of the Boeing 747-100/200 Longitudinal Motion. Ph.D. Thesis, University of Minnesota.

Michalopoulos, P., Yi, P., Lyrintzis, A., 1992. Development of an improved high-order continuum traffic flow model. Transportation Research Record (1365), 125–132.

Papageorgiou, M., 1983. Applications of Automatic Control Concepts to Traffic Flow Modeling and Control. Springer.

Papageorgiou, M., 2003. Handbook of Transportation Science. Traffic Control. Kluwer Academic Publisher (Chapter 8).

Papageorgiou, M., Blosseville, J.-M., Hadj-Salem, H., 1990. Modelling and real-time control of traffic flow on the southern part of Bouleavard Peripherique in Paris: Part I modelling. Part II: coordinated on ramp metering. Transportation Research Part A 24 (5), 345–370.

Papageorgiou, M., Hadj-Salem, H., Blosseville, J.-M., 1991. Alinea: a local feedback control law for on-ramp metering. Transportation Research Record (1320), 58–64.

Payne, H.J., 1971. Models of freeway traffic and control. Simulation Councils Proceedings Series 1, 51–61.

Rugh, W.J., Shamma, J., 2000. Research on gain scheduling. Automatica 36, 1401–1425.

Shamma, J., Athans, M., 1990. Analysis of nonlinear gain scheduled control systems. IEEE Transactions on Automatic Control 35 (8), 898–907.

Shamma, J., Cloutier, J., 1993. Gain scheduled missile autopilot design using linear parameter varying transformation. AIAA Journal of Guidance, Control, and Dynamics 16 (2), 256–263.

Wang, Y., Papageorgiou, M., 2005. Real-time freeway traffic state estimation based on extended Kalman filter: a general approach. Transportation Research Part B 39 (2), 141–167.

Wu, F., 1995. Control of Linear Parameter Varying Systems. Ph.D. Thesis, University of California at Berkeley, Bekeley, USA.